

Polyanionic Polydentate Europium Complexes as Ultrabright One- or Two-photon Bioprobes

Henri Sund, Yuan-Yuan Liao, Chantal Andraud, Alain Duperray, Alexei Grichine, Boris Le guennic, François Riobé, Harri Takalo, Olivier Maury

▶ **To cite this version:**

Henri Sund, Yuan-Yuan Liao, Chantal Andraud, Alain Duperray, Alexei Grichine, et al.. Polyanionic Polydentate Europium Complexes as Ultrabright One- or Two-photon Bioprobes. ChemPhysChem, 2018, 19 (23), pp.3318-3324. 10.1002/cphc.201800557 . hal-01937271

HAL Id: hal-01937271

https://univ-rennes.hal.science/hal-01937271

Submitted on 7 Dec 2018

HAL is a multi-disciplinary open access archive for the deposit and dissemination of scientific research documents, whether they are published or not. The documents may come from teaching and research institutions in France or abroad, or from public or private research centers.

L'archive ouverte pluridisciplinaire **HAL**, est destinée au dépôt et à la diffusion de documents scientifiques de niveau recherche, publiés ou non, émanant des établissements d'enseignement et de recherche français ou étrangers, des laboratoires publics ou privés.

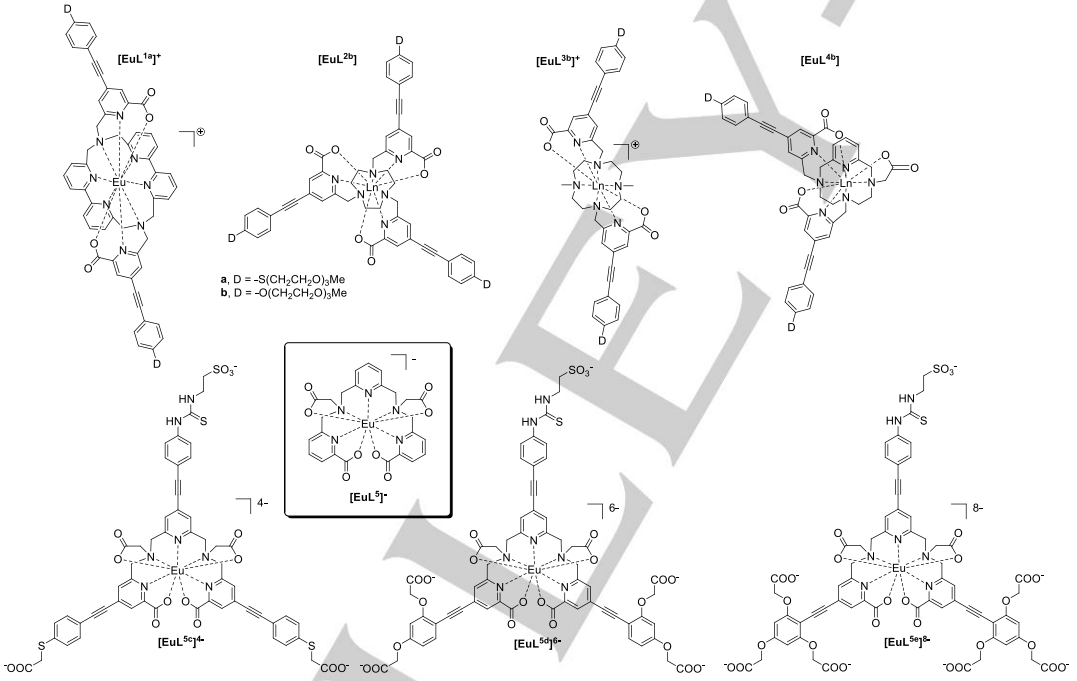
10.1002/cphc.201800557

Polyanionic polydentate europium complexes as Ultrabright one- or two- photon bioprobes.

Henri Sund,[a] Yuan-Yuan Liao,[b] Chantal Andraud,[b] Alain Duperray,[c] Alexei Grichine,[c] Boris Le Guennic,[d] François Riobé,[b] Harri Takalo[a]*, Olivier Maury[b]*

Abstract: A family of europium (III) complexes based on a polydentate ligand functionalized by charge transfer antennae presents remarkable one and two photon photophysical properties in water or buffer. A detailed analysis of their emission properties suggests that the wrapping of the ligand around the central rare-earth ion results in an overall *Cs* symmetry in agreement with the theoretical simulation and that about 65-70% of the emission intensity concentrated in the hypersensitive $^5D_0 \rightarrow {}^7F_2$ transition at 615 nm. Their brightness is excellent, in the range of the best lanthanide bioprobes making them very attractive for bio-imaging experiments.

Figure 1. Structure of existing europium bioprobes (up) and of the studied complexes (bottom).



Introduction

The design of lanthanide luminescent bioprobes (LLBs) for time resolved fluorimetry immunoassay and one or two photon (1P or 2P, respectively) fluorescence microscopy imaging applications is a very active field of research.[1] In this context, the main challenge is to fulfil simultaneously in a single complex a series of requirements:[2] i) the LLB must be kinetically, chemically and photo-chemically stable in complex biological media (culture media, blood, plasma…); (ii) the LLB has to possess a reactive functional group to allow further covalent labelling of a biomolecule but also hydrosolubilizing fragments avoiding non-specific inter-actions;[3] (iii) the 1P-LLB excitation wavelength must be as high as possible, ideally above 330 nm (337 nm correspond to the N_2 laser frequently used as source) to avoid the use of costly quartz optics and enabling 2P excitation in the 700-900 nm spectral range of the Ti:sapphire laser; (iv) the LLB must present the highest 1P-brigthness defined as the product of the molecular absorptivity by the luminescence quantum yield ($B^1 = \varepsilon.\phi$), and/or 2P-brigthness ($B^2 = \sigma^2.\phi$) where ε, $\sigma^2$and ϕ represent the molecular the molecular 1P extinction coefficient, 2P-cross-section and quantum yield, respectively. Consequently the structure of the chelating unit must be carefully chosen to rigorously exclude water molecules from the first coordination sphere and the chromophore antenna must be selected to simultaneously ensure an optimal energy transfer to the central lanthanide emitter and optimise the 1P- and 2P-absorption.[4] During the last decade, charge transfer (CT) antennae became ubiquitous for the design of LLBs because they combined very large extinction coefficient and two-photon cross-section with low energy excitation wavelength due to a direct sensitization mechanism.[5] Using this strategy, extremely bright europium, terbium but also samarium, dysprosium and

[a] M.Sc. Sund, Dr. H. Takalo, Radiometer Turku Oy, Biolinja 12, 20750 Turku, Finland. harrijuha.takalo@gmail.com
[b] Dr. Y.-Y. Liao, Dr. F. Riobé, Dr. C. Andraud, Dr. O. Maury, Univ Lyon, ENS de Lyon, CNRS UMR 5182, Université Claude Bernard Lyon 1, Laboratoire de Chimie, F69342, Lyon, France. olivier.maury@ens-lyon.fr
[c] Dr. A. Grichine, Dr. A. Duperray, Institute for Advanced Biosciences, Inserm U1209, CNRS UMR5309, Université. Grenoble Alpes, 38000 Grenoble, France.
[d] Dr. B. Le Guennic, Univ Rennes, CNRS, ISCR (Institut des Sciences Chimiques de Rennes), UMR 6226, F-35000 Rennes, France

Supporting information for this article is given via a link at the end of the document.

Accepted Manuscript

ytterbium complexes based on the triazacyclononane (TACN) macrocycle have been reported for 1P-or 2P-bioimaging applications.[6] Considering europium, the best antennae are composed of a phenylethynylpyridine chromophore[7] further functionalized by mild electro-donating moieties like alcoxy, thioether or amido ones.[5] Such antennae have been grafted on various macrocycles like bis-bipyridine aza-macrocycle [Eu**L**^{1a}]$^{+}$,[8] TACN [Eu**L**^{2b}],[6,9] cyclen [Eu**L**^{3b}]$^{+}$[10] or pyclen [Eu**L**^{4b}][11a] (Figure 1). In particular, excellent brightness has been obtained in water for [Eu**L**^{2b}] (B^1(337) = 15-30000 L.mol^{-1}.cm^{-1}) and [Eu**L**^{4b}] (B^1(336)= 12300 L.mol^{-1}.cm^{-1}).

In this article, we describe the incorporation of such CT antennae in a polydendate ligand depicted in Figure 1. Two picolinic CT antennas are located at each extremity of the ligand whereas the central pyridine exhibits a thiourea functionality. This fragment comes from a isothiocyanate reactive function which was initially introduced for bioconjugation. To perform the photophysical study, the isothiocyanate was reacted with taurine.[12] The CT antennas are functionalized by one thioether or two alcoxy electrodonating fragments further decorated by carboxylate moieties to ensure hydrosolubility resulting in the formation of tetra, hexa and octa-anionic complexes [Eu**L**^{5c}]$^{4-}$, [Eu**L**^{5d}]$^{6-}$ to [Eu**L**^{5e}]$^{8-}$ respectively. A combined theoretical and photophysical study is presented to determine the symmetry of these complexes in solution; the linear and nonlinear two-photon absorption properties have been evaluated highlighting the excellent 1P-and 2P brightness of this family. Finally, their potential in 2P-microscopy imaging applications has been evaluated.

Results and Discussion

Synthesis. The synthesis of [Na]$_6$[Eu**L**^{5d}] and [Na]$_8$[Eu**L**^{5e}] has been previously described.[12] The preparation of [Na]$_4$[Eu**L**^{5c}] required a similar procedure which is described in SI (Scheme S1).

Geometry optimization of the complexes. The tridimentionnal structure of this class of complexes remains unknown due to the impossibility to obtain monocrystals suitable for X-ray crystallography. This is the case for the π-conjugated antenna functionalized derivatives [Eu**L**^{5c}]$^{4-}$, [Eu**L**^{5d}]$^{6-}$ to [Eu**L**^{5e}]$^{8-}$ but also for the non-functionalized parent complex [Eu**L**^{5}]$^{-}$. Consequently, the geometry of the complexes was investigated using density functional theory (DFT, see computational details in Experimental Section) on yttrium models [Y**L**^{5}]$^{-}$ and [Y**L**^{5c}]$^{-}$ where the charged carboxylate and sulfonate end-groups were replaced with methyl fragments.

The geometry optimisation of [Y**L**^{5}]$^{-}$ indicate the formation of two isomers depending on the wrapping of the polydentate ligand around the central metal ion (Figure 2). In both cases the coordination number is nine and involves 5 nitrogen atoms coming from the central pyridine (N_{py}), the tertiary amine ($2N_a$) and the picolinate ($2N_{pa}$) -and 4 oxygen atoms form the acetate ($2O_{ac}$) and picolinate ($2O_{pa}$) moieties. However, the geometry of the two isomers differs significantly: for the isomer 1, the two picolinates are distributed on each side of a pseudo-equatorial plane formed by the central pyridine, the two tertiary amines and an additional carboxylate. The second acetate completes the coordination sphere. The second isomer differs by the inversion of the configuration of one of the tertiary amine. The pseudo-equatorial plane includes this time one of the picolinate. Thus, the two acetate moities occupy one face of the complex while the second picolinate is in opposition regard to the metal center. The Shape analysis performed on both isomers indicates that resulting coordination polyhedra are close to a C_s symmetry point group (Table S1). Interestingly, isomer 1 was found 0.17 eV (3.98 kcal/mol) more stable than isomer 2. This result is not surprising since the steric hindrance between picolinate fragments is minimized in the case of isomer 1. Consequently, the geometry of the complex [Y**L**^{5c}]$^{-}$ was optimized only for Isomer 1. Interestingly, the wrapping of the ligand around the central metallic ion results in an overall apparent threefold symmetry of the π-conjugated antenna (Figure 3).

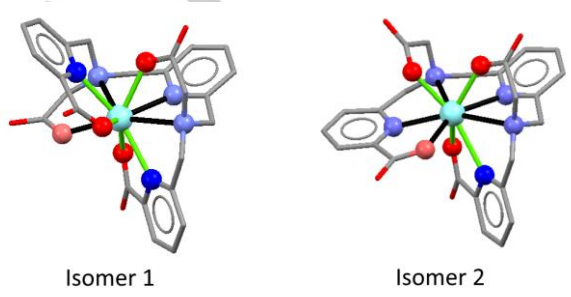


Figure 2. Representation of the DFT optimized geometry of the two isomers of [Y**L**^{5}]$^{-}$. Donor atoms belonging to the pseudo-equatorial plane represented in light colours with black bonds to the Yttrium (light blue). Other coordination bonds are depicted in green.

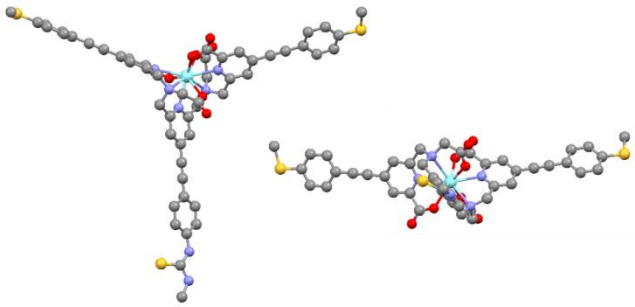


Figure 3. Representation of the DFT optimized geometry of the isomers 1 of [Y**L**^{5c}]$^{-}$.

Absorption and emission spectroscopy. The photophysical characterization of the compounds has been performed in diluted water and Tris buffer solutions and the results are compiled in Table 1. The absorption spectra (Figure 4) are characteristic of charge transfer antennae[5] with a broad intense transition centred around 340 nm. A slight red shift is observed going from [Eu**L**^{5c}]$^{4-}$, [Eu**L**^{5d}]$^{6-}$ to [Eu**L**^{5e}]$^{8-}$ ($\Delta\lambda$ = 6 and 5 nm

Accepted Manuscript

respectively) due to the presence of 1, 2 and 3 electron donor groups in the conjugated antennae reinforcing the charge transfer. Upon excitation in the absorption band, an intense red emission is observed with the characteristic Eu(III) profile assigned to $^5D_0 \rightarrow {}^7F_J$ (J = 0 to 4) transitions (Figure 5). No ligand centred emission remains visible indicating that the sensitization process is very straightforward. Interestingly, due to the broadness of the absorption band ($\lambda_{cut\text{-}off}$ about 400 nm), it is possible to sensitize the Eu(III) luminescence in the visible range, corresponding to the working range of a wide-used LED (λ_{ex} = 405 nm). The quantum yields in water and Tris buffer are high (20-25%) and the lifetimes are relatively long (0.7-0.85 ms) (Table 1) similar to other complexes featuring identical antennae but different structure like TACN [Eu**L**^{2b}] or Pyclen [Eu**L**^{4b}]. Consequently, the one-photon brightness of these complexes is very high 15-20 000 L. Mol^{-1}.cm^{-1} comparable to the best Eu(III) LLBs [6,9,11] and making them particularly attractive for further use in fluoro-immunoassay (with possible excitation at 337 nm) or bio-imaging experiments.

Table 1. Photophysical Data of europium complexes in water or Tris buffer solutions at room temperature.

	λ_{max} (nm) ε (L.mol^{-1}.cm^{-1})	ϕ [a]	τ (ms)	B^1 [b] (L.mol^{-1}. cm^{-1})	σ^2 (GM) λ^2 = 720 nm
[Eu**L**^{5c}]$^{4-}$					
H_2O	336 (65000)	0.25	0.85	16250	47
Tris	*340 (69000)*	*0.20*	*0.77*	*13800*	
[Eu**L**^{5d}]$^{6-}$					
H_2O	342 (91000)	0.28	0.86	25480	75
Tris	*343 (85000)*	*0.18*	*0.84*	*15300*	
[Eu**L**^{5e}]$^{8-}$					
H_2O	349 (64000)	0.19	0.74	12160	58
Tris	*349 (64000)*	*0.26*	*0.70*	*16640*	

[a] quinine bisulfate in H_2SO_4 0.5M as standard (Φ = 54.6%) [b] measured at λ_{max}. …

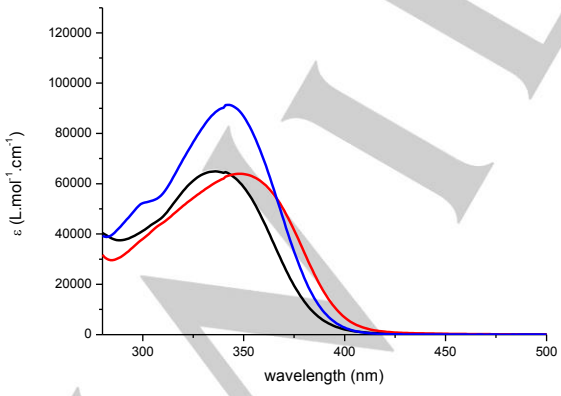


Figure 4. Absorption spectra in water solution at room temperature of [Eu**L**^{5c}]$^{4-}$ (black), [Eu**L**^{5d}]$^{6-}$ (blue) to [Eu**L**^{5e}]$^{8-}$ (red).

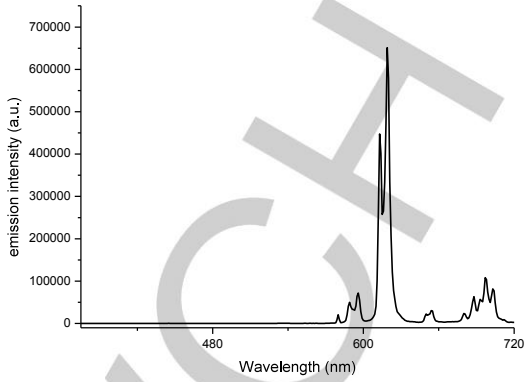


Figure 5. Representative emission spectrum of [Eu**L**^{5c}]$^{4-}$(black), in water solution (excitation at 340 nm) at room temperature.

Solution structure of the europium complexes. It is well known that europium complexes are particularly sensitive to their local environment and their emission spectra are clearly the signature of the complex symmetry in solution. In this context, two main effects can be explored: the crystal-field splitting (CFS) of each transition and their relative intensity, this latter being frequently used for sensing purposes (ie, titration of an analyte using transition intensity variations).

The splitting of each $^5D_0 \rightarrow {}^7F_J$ (J = 0 to 4) transition was studied on the basis of the low temperature (77K) emission spectrum recorded in an organic glass (Figure 6). The resolution is strongly improved due to the reduction of the vibronic broadening of the bands. Importantly, the $^5D_0 \rightarrow {}^7F_0$ transition, insensitive to any CFS effect, can be nicely fitted with a single Gaussian curve indicating the presence of a single emissive species at 77K, in all probability the most stable isomer 1 found by the theoretical calculations. The J=1 and J=4 transitions are now clearly resolved and can be decomposed in three and nine Gaussian curves, respectively (Figure 6). In the hypersensitive J=2 transition the different contributions are merged in 3 main bands. Overall, the splitting of each transition in 2J+1 sub-components is observed, signature of a low symmetry complex according to the CFS theory[13] and in agreement with the theoretical geometry optimization.

In addition, the relative intensity of the $^5D_0 \rightarrow {}^7F_J$ (J = 0 to 4) transition of the different complexes are rather similar (Table S2 and Figure S1). As example [Eu**L**^{5c}]$^{4-}$ presents an emission profile with relative intensity of 0.1, 1, 10.9, 0.5 and 3.1 using the J=1 magnetic dipole transition as internal reference.[13] In order to envisage further applications of these complexes as FRET-donors it is important to minimize the intensity of the J=4 transition, that generally overlaps with the emission of the FRET-acceptor dye. For convenience, we defined the r value as the ratio of the intensity of the J=2 over J=4 transition and this parameter is an indicator to compare the symmetry of different complexes. As a general tendency, highly symmetrical

Accepted Manuscript

complexes exhibit very intense J=2 transition and weak J=4 ones hence high r value.[13] In the present cases the three complexes [Eu**L**^{5c}]$^{4-}$, [Eu**L**^{5d}]$^{6-}$ and [Eu**L**^{5e}]$^{8-}$ present similar r values comprised between 2.8 and 3.5 with an hypersensitive transition representing R^2 = 65-70% of the whole emission spectrum (Table 2). This value is lower than that of the TACN based complex [Eu**L**^{2b}][6,9] (r = 10.9, R^2 = 79%) featuring an almost perfect threefold symmetry but higher than that of other macrocyclic compounds like cyclen [Eu**L**^{3b}]$^{+}$ (r = 2.5, R^2 = 56%) [10] or pyclen [Eu**L**^{4b}] [11] (r = 3.0, R^2 = 65%) featuring C_{2v} and distorted C_3 symmetry, respectively.

Table 2. Photophysical parameters determined from the complexes room temperature emission spectra in water.[a]

	r	R^2 (%)	R^1 (%)	τ_{rad} (ms)	ϕ_{Eu}	k_{rad} (s^{-1})	Σk_{nr} (s^{-1})
[Eu**L**^{5c}]$^{4-}$	3.5	69.8	0.06	1.99	0.43	502.9	673.6
[Eu**L**^{5d}]$^{6-}$	2.8	65.5	0.07	2.13	0.40	468.7	694.1
[Eu**L**^{5e}]$^{8-}$	3.5	69.6	0.06	2.01	0.37	498.7	852.6

[a] $r = I_{J=2}/I_{J=4}$, $R^2 = I_{J=2}/I_{tot}$; $R^1 = I_{J=1}/I_{tot}$; $k_{rad} = 1/\tau_{rad} = A(0,1).n^3/R^1$ where A(0,1) is the spontaneous emission probability in vacuum determined to 14.65 s^{-1} and n is the refractive index of water equal to 1.333; $\phi_{Eu} = \tau/\tau_{rad} = k_{rad}/(k_{rad}+\Sigma k_{nr})$

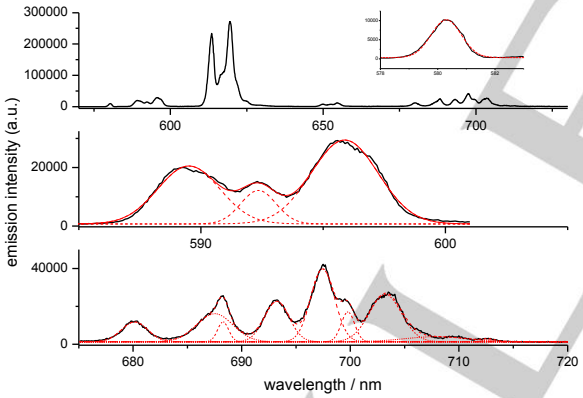


Figure 6. 77K emission spectra of [Eu**L**^{5c}]$^{4-}$(black) in organic glass (MeOH/EtOH, 1/4, v/v) under 370 nm excitation with optimal resolution (detection slit 0.2, increment 0.2 nm). (Top) full spectra, in inset is represented the magnification of the J=0 transition emission spectrum with a single Gaussion deconvolution (red). (Middle) Magnification of the J=1 transition and decomposition in three Gaussian curves (dashed red, sum in red). (Bottom) Magnification of the J=4 transition and decomposition in nine Gaussian curves (dashed red, sum in red).

Two-photon absorption properties. The emission of [Eu**L**^{5c}]$^{4-}$, [Eu**L**^{5d}]$^{6-}$ and [Eu**L**^{5e}]$^{8-}$ is intense enough to measure the two-photon properties of these complexes using the two-photon excited fluorescence (TPEF) method in water. The set-up description is given in the experimental section. Upon 2P-

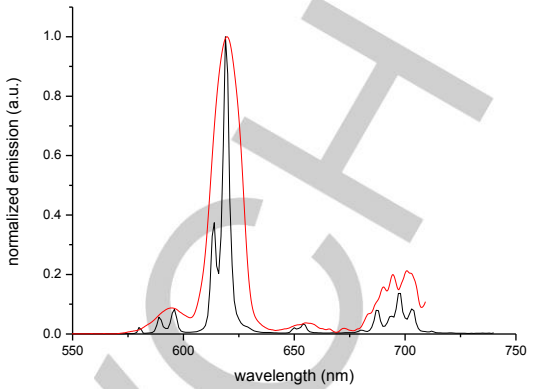


Figure 7. 1P-(red) and 2P-(blue) excited luminescence spectra of [Eu**L**^{5c}]$^{4-}$ at room temperature in water with excitation at 345 and 810 nm, respectively. The spectral resolution difference is du to the different experimental setup (see experimental section for details).

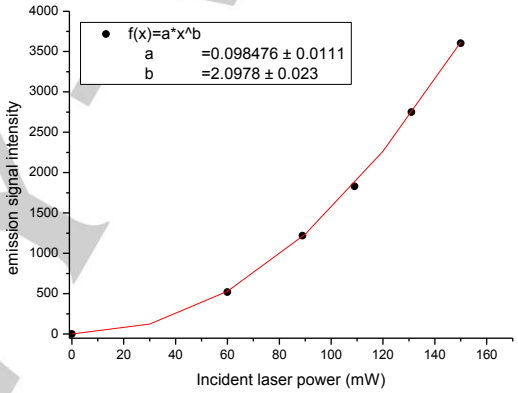


Figure 8. Variation of the Eu(III) luminescence intensity with the laser excitation of [Eu**L**^{5c}]$^{4-}$ in water (2P-excitation λ_{ex} = 760 nm, ●). The red line represents the fitting of the experimental points by the polynomial function indicated in inset.

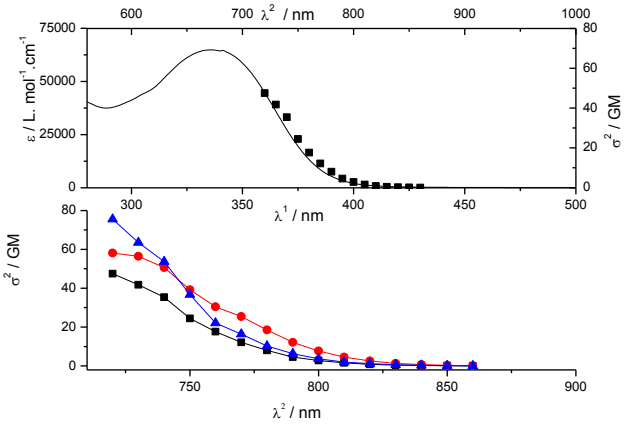


Figure 9. (Top) 1P-absorption spectrum of [Eu**L**^{5c}]$^{4-}$in water at RT (black line, lower abscissa). Superimposed on this plot is the 2P-absorption measured by TPEF method in water in wavelength doubled scale (■, upper abscissa). (bottom) 2P-absorption spectra of [Eu**L**^{5c}]$^{4-}$(■), [Eu**L**^{5d}]$^{6-}$ (▲) to [Eu**L**^{5e}]$^{8-}$ (●).

Accepted Manuscript

excitation at 810 nm, the europium emission is detected (Figure 7) and its profile looks similar to that obtained under classical 1P-excitation in spite of a lower spectral resolution due to the experimental set-up. Furthermore, the intensity of Eu(III) emission displays a quadratic variation with the incident laser power, unambiguously illustrating the 2P-antenna effect in water (Figure 8). Finally, the 2P-cross sections have been measured in water using coumarin-307 as external standard (Figure 9). Since the complex did not present any inversion center, it is not surprising to observe a perfect correspondence between the 2P-absoprtion spectrum and the wavelength-doubled 1P-one (Figure 9). This result clearly indicated that the low lying CT state is responsible for the Eu(III) sensitization under 1P- and 2P excitation. The 2P-cross-sections of the three complexes ranged between 50-100 GM which are classical values for this type of antennae.[14] It is worth noting that, due to the spectral limitation of the incident laser source (700-900 nm), the 2P-maximum is not reached and only the red tail of the 2P-spectrum is observed. Nevertheless, one can notice that the 2P-cross-sections at 720 nm increase with the increase of the CT character of the antenna.

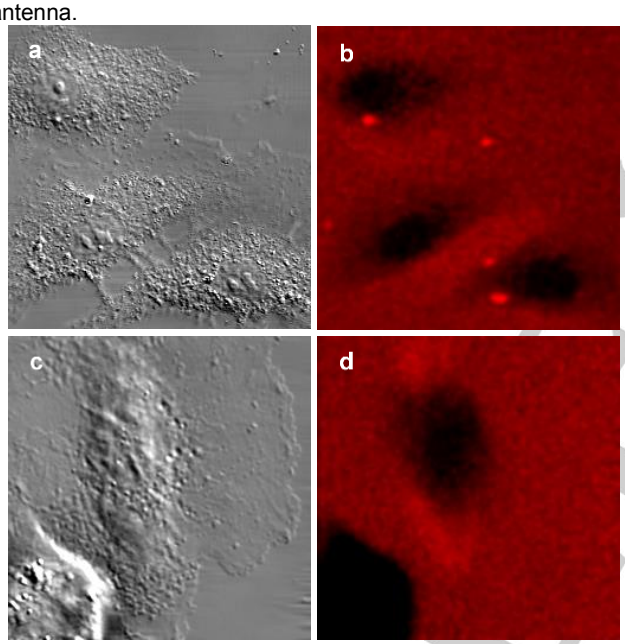


Figure 10. 2P imaging of living T24-cells stained with [Eu**L**^{5c}]$^{4-}$ (b) and [Eu**L**^{5e}]$^{8-}$ (d). (λ_{exc} = 780 nm). In (a) and (c) the corresponding transmitted light DIC images are represented. Complexes are added in the cell medium in phosphate buffer solution to reach a final concentration of 5-10 10^{-6} mol.L^{-1}.

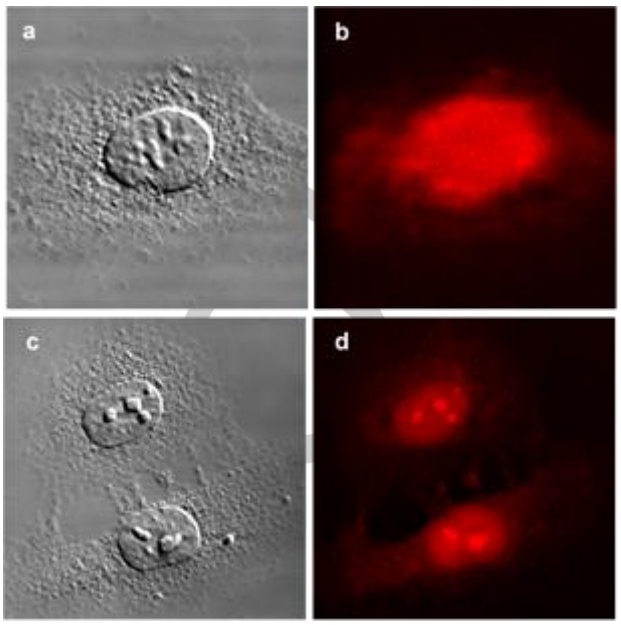


Figure 11. 2P imaging of (PFA)-fixed T24-cells (a, c) stained with [Eu**L**^{5c}]$^{4-}$ (b) and [Eu**L**^{5e}]$^{8-}$ (d). (λ_{exc} = 780 nm). In (a) and (c) the corresponding transmitted light DIC images are represented. Complexes are added in the cell medium in phosphate buffer solution to reach a final concentration of 5-10 10^{-6} mol.L^{-1}.

Two-photon microscopy imaging. The complexes [Eu**L**^{5c}]$^{4-}$, and [Eu**L**^{5e}]$^{8-}$ were then involved in 2P-bioimaging experiments using T24 cells (staining concentration of 5-10 10^{-6} mol.L^{-1}). The experiment was first performed with living cells (Figure 10). In our hands, it appears clearly that the two complexes did not cross the plasma membrane and remained in the culture medium, the cells appearing as dark areas. Such behaviour is typically observed for anionic complexes and is generally explained by an electrostatic repulsion with the negatively charged membrane surface especially inner leaflet of the lipid bi-layer and glycocalix.[15] The cells were then fixed with paraformaldehyde (PFA) and treated with Triton X-100 to increase their permeability. Mild PFA fixation is known to preserve the native shape of biological structures keeping them hydrated. In this case, the complexes are internalized and fixed to some specific area in the cells. This is particularly visible for the [Eu**L**^{5e}]$^{8-}$ complex that clearly accumulates in the nucleus and to less extent the endoplasmic reticulum and mitochondrial network (Figure 11). In particular the brightest spots in the nucleus correspond to nucleoli. This behavior has already been described for related tris anionic trisdipicolinate complexes.[16] The luminescence spectrum of [Eu**L**^{5e}]$^{8-}$ *in cellulo* was monitored and presented the characteristic Eu(III) emission profile (Figure S2). Finally the luminescence lifetime was measured in fixed cells using the TSLIM method[17] and a rather short lifetime of ca 0.44 ms was found (Figure S3). This value is shorter than that found in water (0.74), in Tris buffer (0.70 ms) or after bio-conjugation to IgG (0.69).[12] This lifetime decrease can be explained by an increased fluxionality of the complex in the biological environment containing a complex mixture of salts or biomacromolecules.

Accepted Manuscript

Conclusions

In conclusion, this family of europium (III) complexes based on polydentate CT functionalized ligand presents excellent 1P- and 2P-brigthness in water and buffer making them suitable for bio-imaging experiments. A careful photophysical study suggests that the wrapping of the ligand around the central rare-earth ion results in an overall threefold symmetry with about 65-70% of the emission intensity concentrated in the hypersensitive $^5D_0 \rightarrow {}^7F_2$ transition at 615 nm. These remarkable linear and nonlinear photophysical properties, combined with the presence of a reactive function in the central pyridine moieties make these complexes particularly attractive for further use as LLBs in fluoroimmunoassay.

Experimental Section

Photophysical measurements in solution. Absorption spectra were recorded on a JASCO V-650 spectrophotometer as solutions in spectrophotometric-grade methanol or water (ca. 10^{-5} or 10^{-6} mol.L^{-1}). Emission spectra were measured using a Horiba–Jobin–Yvon Fluorolog-3 fluorimeter. Spectra were corrected for both excitation-source light-intensity variation and emission spectral responses. Luminescence lifetimes were obtained by pulsed excitation with a FL-1040 UP xenon lamp. Luminescence quantum yields, Φ, were measured with dilute solutions in water or organic solvents with an absorbance of less than 0.1 by using equation (1):

$$\frac{\Phi_x}{\Phi_r} = \frac{A_r(\lambda)}{A_x(\lambda)} \frac{{n_x}^2}{{n_r}^2} \frac{D_x}{D_r} \quad (1)$$

in which A is the absorbance at the excitation wavelength (λ), n is the refractive index, and D is the integrated luminescence intensity; r and x stand for reference and sample, respectively The reference is quinine bisulfate in a 1N aqueous solution of sulfuric acid (Φ_r = 0.546). Excitation of reference and sample compounds was performed at the same wavelength. Practically, for each sample, series of measurements are performed with different absorbance ranging from 0.1 to 0.01. The plot of the integrated luminescence intensity vs. absorbance gives straight line with excellent correlation coefficients and the slope *S* can be determined. Equation (1) becomes (2):

$$\frac{\Phi_x}{\Phi_r} = \frac{S_x(\lambda)}{S_r(\lambda)} \frac{{n_x}^2}{{n_r}^2} \quad (2)$$

Two-photon excited luminescence measurements. The TPA cross-section spectrum was obtained by up-conversion luminescence using a Ti:sapphire fs laser in the range 700-900 nm. The excitation beam (5 mm diameter) is focalized with a lens (focal length 10 cm) at the middle of the 10-mm cell. Emitted light was collected at 90° and was focused into an optical fiber (diameter 600 μm) connected to an Ocean Optics S2000 spectrometer. The incident beam intensity was adjusted to 50 mW in order to ensure an intensity-squared dependence of the luminescence over the whole spectral range. The detector integration time was fixed to 1s. Calibration of the spectra was performed by comparison with the published 700-900 nm Coumarin-307 two-photon absorption spectrum[18] (luminescence quantum yield = 0.56 in ethanol). The measurements were done at room temperature in dichloromethane and at a concentration of 10^{-4} M.

Cell culturing and treatment. We used the T24 human epithelial bladder cancer cell line (ATCC no. HBT-4). In our experiments, T24 cells were cultured in 25 cm^2 tissue-culture flasks (T25) at 37°C in a humidified atmosphere with 5% CO_2. They were incubated in RPMI 1640 supplemented with 100 UmL^{-1} penicillin, 100 µg.mL^{-1} streptomycin, and 10% fetal calf serum (complete medium). Cells were grown to near confluence in the culture flasks and then suspended with a solution of 0.05% trypsin–ethylenediaminetetraacetic acid (EDTA; Sigma). Cells were placed on a LabTek I chambered cover glass (Nunc) at low cell density in complete culture medium 24 h before experiments. After being washed with phosphate-buffered saline (PBS), cells were fixed with PFA (3% in PBS) for 10 min, permeabilized with PBS containing 0.5% Triton X100 for 10 min, and then washed with PBS. The staining is performed by addition of a concentrated solution of complex (10^{-4} mol.L^{-1}) in PBS buffer to the cell culture medium to reach a final concentration of 5-10 10^{-6} mol.L^{-1}.

Confocal and two-photon microscopy. All confocal experiments were performed using a LSM710 NLO (Carl Zeiss) confocal laser scanning microscope based on the inverted motorized stand (AxioObserver, Zeiss). The excitation was provided by either 561 nm DPSS cw laser or Ti:Sa femtosecond tuneable laser (Chameleon, Ultra II, Coherent) for 2P excitation at 750 nm in descanned detection mode. In the former case the pinhole was closed to 1 Airy Unit and in the latter one it was fully open. Spectral imaging was realized using an internal Quasar detector in the range 577-723 nm with the resolution of 9.7 nm.

Computational details. DFT geometry optimizations were carried out with the Gaussian 09 (Revision D.01)[19] package employing the PBE0 hybrid functional[20] and tightening self-consistent field convergence thresholds (10-10 a.u.) and geometry optimization (10-5 a.u.) convergence thresholds. The “Stuttgart/Dresden” basis sets and effective core potentials were used to describe the yttrium atom,[21] whereas all other atoms were described with the SVP basis sets.[22] The analysis of the calculated symmetry was performed with the Shape program.[23]

Acknowledgements

B.L.G. thanks the French GENCI-CINES centre for high-performance computing resources. Confocal and 2P facility of the IAB platform was co-funded thanks to grants of “Association pour la Recherche sur le Cancer”, Ligue Contre le Cancer, and the CPER program.

Keywords: Europium • Luminescence • Bioprobe • Two-photon microscopy • Bioimaging

References

[1] a) C. P. Montgomery, B. S. Murray, E. J. New, R. Pal, D. Parker, *Acc. Chem. Res*. **2009**, *42*, 925-937; b) E. G. Moore, A. P. S. Samuel, K. N. Raymond, *Acc. Chem. Res*. **2009**, *42*, 542-552; c) E. J. New, D. Parker, D. G Smith, J. W Walton *Curr. Opin. Chem. Biol*. **2010**, 14, 238-246; d) A. D’Aléo, C. Andraud and O. Maury, *Luminescence of Lanthanide Ions in Coordination Compounds and Nanomaterials* Ed. A. De Bettencourt-Diaz), Wiley **2014**, 197-226; J.-C. G. Bünzli, ibd pp 125-196; e) M. Rajendran, E. Yapici, L. W. Miller, *Inorg. Chem. (Forum Article)* **2014**, *53*, 1839−1853 ; f) M. Sy, A. Nonat, N. Hildebrandt, L. J. Charbonnière *Chem. Commun*., **2016**, *52*, 5080-5095.

[2] J.-C. G. Bünzli, *Chem. Rev.*, **2010**, *110*, 5, 2729-2755.

[3] V. Placide, D. Pitrat, A. Grichine, A. Duperray, C. Andraud, O. Maury *Tetrahedron Lett.* **2014**, *55*, 1357–1361.

[4] a) M. Latva, H. Takalo, V.-M. Mukkala, C. Matachescu, J.C. Rodríguez-Ubis, J. Kankare, *J. Lumin*., **1997**, *75* 149-169; b) S. V. Eliseeva, J.-C.

Accepted Manuscript

G. Bünzli *Chem. Soc. Rev.* **2010**, *39*, 189-227; c) A. D'Aléo, L. Ouahab, C. Andraud, F. Pointillart, O. Maury, *Coord. Chem Rev.* **2012**, *256*, 1604-1620; d) J.-C. Bünzli, *Coord. Chem. Rev*. **2015**, *293-294*, 19-47.

[5] a) C. Yang, L.-M. Fu, Y. Wang, J.-P. Zhang, W.-T. Wong, X.-C. Ai, Y.-F. Qiao, B.-S. Zou, L.-L. Gui, *Angew. Chem., Int. Ed.* **2004**, *43*, 5010-5013; b) A. D'Aléo, A. Picot, A. Beeby, J.A. G. Williams, B. Le Guennic, C. Andraud, O. Maury, *Inorg. Chem*., **2008**, *47*, 10258-10268.

[6] a) A. D'Aléo, A. Bourdolle, S. Bulstein, T. Fauquier, A. Grichine, A. Duperray, P. L. Baldeck, C. Andraud, S. Brasselet, O. Maury *Angew. Chem. In. Ed.* **2012**, *51*, 6622 –6625; b) J. W. Walton, A. Bourdolle, S.J. Butler, M. Soulier, M. Delbianco, B.K. McMahon, R. Pal, H. Puschmann, J.M. Zwier, L. Lamarque, O. Maury, C. Andraud, D. Parker *Chem. Commun.* **2013**, *49*, 1600-1602; c) A. T. Bui, A. Grichine, S. Brasselet, A. Duperray, C. Andraud, O. Maury *Chem. Eur. J.* **2015**, *21*, 17757-17761; d) A. T. Bui, A. Roux, A. Grichine, A. Duperray, C. Andraud, O. Maury *Chem. Eur. J.* **2018**, *24*, 3408-3412.

[7] a) J. Kankare, M. Latva, H. Takalo, *Eur. J. Solid. State Inorg. Chem.* **1991**, *28*, 183-186; b) H. Takalo, E. Hänninen, J. Kankare, *Helv. Chim. Acta*, **1993**, *76*, 877-883.

[8] A. Bourdolle, M. Allali, J.-C. Mulatier, B. Le Guennic, J. Zwier, P. L. Baldeck, J.-C.G. Bünzli, C. Andraud, L. Lamarque and O. Maury *Inorg. Chem*. **2011**, *50*, 4987-4999.

[9] a) M. Soulié, F. Latzko, E. Bourrier, V. Placide, S. J. Butler, R. Pal, J. W. Walton, P. L. Baldeck, B. Le Guennic, C. Andraud, J. M. Zwier, L. Lamarque, D. Parker and O. Maury *Chem. Eur. J.* **2014**, *20*, 8636–8646; b) M. Delbianco, V. Sadovnikova, E. Bourrier, G. Mathis, L. Lamarque, J. M. Zwier, D. Parker *Angew. Chem., Int. Ed.*, **2014**, *53*, 10718-10722.

[10] a) A. T. Bui, M. Beyler, Y.-Y. Liao, A. Grichine, A. Duperray, J.-C. Mulatier, B. Le Guennic, C. Andraud, O. Maury and R. Tripier, *Inorg. Chem.*, **2016**, *55*, 7020-7025; b) A. D'Aléo, M. Allali, A. Picot, P. L. Baldeck, L. Toupet, C. Andraud, O. Maury *C. R. Chimie* **2010**, *13*, 681-690.

[11] a) N. Hamon, M. Galland, M. Le Fur, A. Roux, A. Duperray, A. Grichine, C. Andraud, B. Le Guennic, M. Beyler, O. Maury, R. Tripier *Chem. Commun.* **2018**, *54*, 6173 – 6176; b) A.-S. Chauvin, S. Comby, B. Song, C. D. B. Vandevyver, J.-C. G. Bünzli *Chem. Eur. J.*, **2008**, *14*, 1726-1739.

[12] H. Sund, K. Blomberg, N. Meltola, H. Takalo *Molecules* **2017**, *22*, 1807.

[13] a) S. V. Eliseeva, J.-C. G. Bünzli, in *Chap 1 Springer series on fluorescence, Vol. 7, Lanthanide spectroscopy, Materials, and Bio-applications, ed. P; Hännen and H. Härmä, Springer Verlag, Berlin, Vol. 7*, **2010**; 1; b) P. A. Tanner *Chem. Soc. Rev.* **2013**, *42*, 5090-5101; c) K. Biennemans *Coord. Chem. Rev.* **2015**, *295*, 1-45.

[14] a) C. Andraud, O. Maury, *Eur. J. Inorg. Chem.*, **2009**, 4357-4371; b) Y. Ma, Y. Wang, *Coord. Chem. Rev.*, **2010**, *254*, 972-990.

[15] a) E. J; New, D. Parker, D. G. Smith, J. W. Walton, *Curr. Op. Chem. Biol.* **2010**, *14*, 238–246; b) S. J. Butler, B.K. McMahon, R. Pal, D. Parker, J. W. Walton, *Chem. Eur. J.* **2013**, 19, 9511-9517; c) E. Deiters, B. Song, A.-S. Chauvin, C. D. B. Vandevyver, F. Gumy J.-C. G. Bünzli, *Chem. Eur. J.*, **2009**, *15*, 885-900; d) A. T. Bui, M. Beyler, A. Grichine, A. Duperray, J.-C. Mulatier, C. Andraud, R. Tripier, S. Brasselet, O. Maury *Chem. Commun.* **2017**, *53*, 6005-6008.

[16] A. Picot, A. D'Aléo, P.L. Baldeck, A. Grishine, A. Duperray, C. Andraud, O. Maury *J. Am. Chem. Soc.* **2008**, *130* (5), 1532-1533.

[17] A. Grichine, A. Haefele, S. Pascal, A. Duperray, R. Michel, C. Andraud, O. Maury *Chem. Science*, **2014**, *5*, 3475-3485.

[18] C. Xu, W. W. Webb, J. *Opt. Soc. Am. B* **1996**, *13*, 481-491.

[19] Gaussian 09, Revision D.01, M. J. Frisch, G. W. Trucks, H. B. Schlegel, G. E. Scuseria, M. A. Robb, J. R. Cheeseman, G. Scalmani, V. Barone, B. Mennucci, G. A. Petersson, H. Nakatsuji, M. Caricato, X. Li, H. P. Hratchian, A. F. Izmaylov, J. Bloino, G. Zheng, J. L., Sonnenberg, M. Hada, M. Ehara, K. Toyota, R. Fukuda, J. Hasegawa, M. Ishida, T. Nakajima, Y. Honda, O. Kitao, H. Nakai, T. Vreven, J. A. Montgomery, Jr., J. E. Peralta, F. Ogliaro, M. Bearpark, J. J. Heyd, E. Brothers, K. N. Kudin, V. N. Staroverov, T. Keith, R. Kobayashi, J. Normand, K. Raghavachari, A. Rendell, J. C. Burant, S. S. Iyengar, J. Tomasi, M. Cossi, N. Rega, J. M. Millam, M. Klene, J. E. Knox, J. B. Cross, V. Bakken, C. Adamo, J. Jaramillo, R. Gomperts, R. E. Stratmann, O. Yazyev, A. J. Austin, R. Cammi, C. Pomelli, J. W. Ochterski, R. L. Martin, K. Morokuma, V. G. Zakrzewski, G. A. Voth, P. Salvador, J. J. Dannenberg, S. Dapprich, A. D. Daniels, O. Farkas, J. B. Foresman, J. V. Ortiz, J. Cioslowski, D. J. Fox, Gaussian, Inc., Wallingford CT, 2013.

[20] a) J. P. Perdew, K. Burke, M. Ernzerhof, *Phys. Rev. Lett.* **1996**, *77*, 3865–3868; b) C. Adamo, V. Barone, *J. Chem. Phys*. **1999**, *110*, 6158-6170.

[21] M. Dolg, H. Stoll, H. Preuss, *Theor. Chim. Acta* **1993**, *85*, 441-450.

[22] F. Weigend, R. Ahlrichs, *Phys. Chem. Chem. Phys*. **2005**, *7*, 3297-3305.

[23] M. Llunell, D. Casanova, J. Cirera, J. M. Bofill, P. Alemany, S. Alvarez, SHAPE, version 2.1, Barcelona, 2013.

Accepted Manuscript

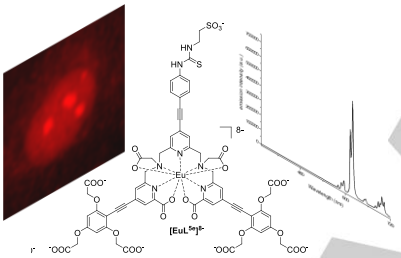
10.1002/cphc.201800557

Entry for the Table of Contents (Please choose one layout)

Layout 1:

ARTICLE

A family of europium (III) complexes based on polydentate ligand functionalized by charge transfer antennae presents remarkable one and two photon photophysical properties in water excellent brightness suitable for bio-imaging applications.



H. Sund, Y.-Y. Liao, C. Andraud, A. Duperray, A. Grichine, B. Le Guennic, F. Riobé, H. Takalo, O. Maury**

Page No. – Page No.

Polyanionic polydentate europium complexes as bright one- or two-photon bioprobe

WILEY-VCH

Accepted Manuscript